Journal of Hazardous Materials 161 (2009) 1208–1215

Contents lists available at ScienceDirect

Journal of Hazardous Materials

journal homepage: www.elsevier.com/locate/jhazmat

Pyrolysis treatment of oil sludge and model-free kinetics analysis

Jianguo Liu, Xiumin Jiang*, Lingsheng Zhou, Xiangxin Han, Zhigang Cui

School of Mechanical Engineering, Shanghai JiaoTong University, Shanghai 200240, PR China

ARTICLE INFO

Article history:
Received 4 January 2008
Received in revised form 26 March 2008
Accepted 19 April 2008
Available online 24 April 2008

Keywords:
Pyrolysis
Oil sludge
Hydrocarbons evolution
Model-free kinetics analysis

ABSTRACT

Pyrolysis of tank bottom oil sludge was investigated to summarize the pyrolysis characteristics through analyzing the change of mass loss, pyrolysis gas compositions in heating process. For this propose, various approaches including thermogravimetric analysis (TGA), CNHS/O elemental analysis, electrically heated fixed bed quartz reactor coupled with Vario Plus emission monitoring system, and oil-gas evaluation workstation (OGE-II) equipped with a flame ionization detector (FID) were used. The pyrolysis reaction is significant in the range of 473–773 K where multi-peak DTG curves can be gained. Higher heating rate increases the carbon (C) and sulfur (S) contents but decreases hydrogen (H) content in solid residues. The major gaseous products excluding N_2 are CHs (Hydrocarbons), CO_2, H_2, CO. The yield of CHs is significant in the range of 600–723 K. Higher heating rate causes the peak intensity of CHs evolution to increase and the CHs evolution to move towards a high-temperature region. Around 80% of total organic carbon content (TOC) in oil sludge can be converted into CHs in pyrolysis process. The CHs data were used for kinetic analysis by Vyazovkin model-free iso-conversion approach. Dependences of the activation energy on the degree of conversion obtained from different methods were compared.

1. Introduction

In the petroleum refineries, a considerable quantity of oil sludge accumulates from refining processes. The major sources of the oil sludge include the oil storage tank sludge, the biological sludge, the dissolved air flotation (DAF) scum. In China, most of the oil sludge is from the treating process of cleaning of oil storage tanks, more than 1 000 000 tones of this kind of sludge are generated annually. Oil sludge is designated as hazardous waste in Resource Conservation and Recovery Act (RCRA) [1], and represents a major source of several contaminants that pollute the soil and the ground water (e.g. petroleum hydrocarbons, metals), and the air (e.g. volatile organic carbons). Typically, oil sludge can be handled via microbial degradation and/or recycling into reusable oils. However, it has been found that such methods cause secondary pollutants. Recently, with its unique characteristic to break down large molecules into smaller ones, pyrolysis has been proven to be an alternative for disposal of this sludge. Using such a process can not only minimize the solid waste but also yield valuable products.

Punnaruttanakun et al. [2] have studied the kinetic and thermal conversion behaviors of API separator oil sludge pyrolysis at different heating rates by TGA. A series of studies on the pyrolysis of oil sludge using TGA has been carried out by Shie et al. [3–9]. They have investigated the major products obtained from the pyrolysis of oil sludge and the pyrolysis properties of oil sludge with catalytic additives by TGA. The research by Wang et al. [10] has shown that pyrolysis reaction of oil sludge starts at a low temperature of about 473 K and the maximum evolution rate was observed between the temperatures of 623 and 773 K by using TG/MS. Schmidt and Kaminsky [11] has pyrolyzed oil sludge in a fluidized bed at temperatures from 733 to 823 K. They found that about 70–84% of the oil could be separated from the solids.

The pyrolysis kinetics study is important to know the decomposition mechanism, rate of reaction, reaction parameters and to predict the products distribution. This in turn helps in proper selection of reactor, optimization of the reactor design and operating conditions. The kinetics of pyrolysis of oil sludge was studied by different authors [2,3,12]. All of them applied model-fitting methods to try to predict pyrolysis process. However the researches have demonstrated that the model-fitting method applied to isothermal data gives rise to unambiguous values of Arrhenius parameters that are likely to conceal multi-step kinetics; and to non-isothermal data always gives rise to highly ambiguous kinetic triplets. This ambiguity ultimately causes the failures of interpretation and utilization of the kinetic triplets [12]. A viable alternative to the model-fitting method is the model-free isoconversional method. Unlike the model-fitting method, which yields a single effective value of the activation energy for the whole process, the isoconversional method has the ability to reveal complexity of the process in the form of a functional dependence of the activation energy (E_α)

* Corresponding author. Tel.: +86 21 3420 5681; fax: +86 21 3420 5681.
E-mail address: xiuminjiang@sjtu.edu.cn (X. Jiang).

0304-3894/$ – see front matter © 2008 Elsevier B.V. All rights reserved.
doi:10.1016/j.jhazmat.2008.04.072

Nomenclature

AAPD	average absolute percentage deviation defined by Eq. (7) (%)
ARD	average relative deviation defined by Eq. (9) (%)
CHs	hydrocarbons evolved in pyrolysis
E_α	activation energy at a given conversion (kJ/mol)
$E_{\alpha,i}^{\text{app}}$	activation energies calculated by approximations of temperature integral (kJ/mol)
$E_{\alpha,i}^{\text{num}}$	activation energies calculated by direct temperature integral (kJ/mol)
k_0	pre-exponential factor (K^{-1})
N	the number of data points for each experiment
R	gas constant (kJ/mol/K)
RD	relative deviation defined by Eq. (6) (%)
t	time (min)
T	temperature (K)
$T_{\alpha,i}$	temperature corresponding to a given conversion of reaction at heating rate β_i (K)
$T_{\alpha,i}^{\text{exp}}$	the experimental value of the temperature at a given α (K)
$T_{\alpha,i}^{\text{pre}}$	the prediction of temperature at which the given α is reached (K)
T_{m}	temperatures corresponding to the peak intensity of CHs evolution (K)
TOC	total organic carbon
W	CHs weight at any temperature T (mg)
W_∞	final evolved CHs weight (mg)

Greek letters

α	conversion of reaction W/W_∞
β	heating rate (K/min)

on the extent of conversion (α). The model-free isoconversional method allows for unmistakably detecting multi-step kinetics as a dependence of E_α on α. Furthermore, it was shown that revealing the dependence of E_α on α not only helps to disclose the complexity of a process, but also helps to identify its kinetic scheme [13–16]. It is well known that oil sludge is a very complex mixture. A quite intricate pyrolysis mechanism of oil sludge in turn can be expected, so the model-free isoconversional method might be more suitable to obtain its kinetics than the model-fitting method.

The information on pyrolysis of oily sludge has been still very limited so far. Detailed information about pyrolysis products, especially the yield of hydrocarbon, during heating process of the sludge is still under way. The present paper aims to evaluate the pyrolysis process and yield of CHs under different heating conditions. The effects of heating rate on pyrolysis process and yield of hydrocarbon were discussed. A Vyazovkin model-free isoconversion approach [17–24] was applied to obtain the kinetic parameters of the oil sludge using some popular temperature integral approximations such as Coats and Redfern [25], Gorbachev [26], Agrawal [27], Li [28], Starink [29] approximations and a new approximation by Cai et al. [30]. The results from the different approximations were compared with that from direct integration [24]. The obtained E_α dependencies derived from non-isothermal data were used to simulate another non-isothermal kinetics data.

2. Experimental

2.1. Samples

The oil sludge sample used in this work was generated from tanker cleaning processes from Shengli Oil Field, Shandong province, northern China. 'As-received' sample appears to be black, viscous and in the form of semi-solid cake at ambient temperature. The proximate analysis and ultimate analysis of the as-received oil sludge are given in Table 1. The heating value of the sample measured by employing a bomb calorimeter is also listed in Table 1. As seen from Table 1, the as-received oil sludge sample has moderate moisture, higher volatile matter, higher ash content and very lower fixed carbon.

2.2. The components of oil sludge

The contents and group composition of chloroform extract on the oil sludge are shown in Table 2. Table 2 shows that the oil sludge contains 26.07 wt.% of chloroform extractable including bituminous (3.32%), satisfied hydrocarbons (11.80%), aromatic hydrocarbons (5.44%) and non-hydrocarbons (5.51%). The use of residue after treatment depends on the heavy metal content. The inorganic materials of the oil sludge were analyzed by an Inductively Coupled Plasma Atomic Emission Spectrometry (ICP/AES) after the chloroform extraction, the total concentration of the metals are listed in Table 3. The quantities of heavy metals (As, Cd, Cr, Cu, Co, Ni, Pb and Zn) in the oil sludge are coincidental to the Chinese environmental quality secondary standard for soils (GB 15618–1995) [31]. So the inorganic materials of the oil sludge can be safely used for farming, if the oil sludge is effectively treated in reducing the concentration levels of petroleum contaminants. The total organic carbon content (TOC) of the oil sludge was determined by a LECO model WR-112 Carbon Determinator, the date of

Table 1
Proximate and ultimate analysis of the oil sludge[a]

Proximate analysis[b] (wt.%)					Element analysis (wt.%)					Net calorific value (kJ/kg)
A	V	FC	M	Comb	C	H	N	S	O[c]	
51.99	28.94	2.12	16.95	31.06	20.85	2.70	0.11	1.40	6.00	8530

[a] Wet basis.
[b] A = ash content, V = volatile matter, FC = fixed carbon, M = moisture, Comb = volatile + fixed carbon.
[c] By difference.

Table 2
Main organic chemical composition of the oil sludge (wt.%)

Organic materials in oil sludge	Chemical composition of organic materials				
	Bituminous	Satisfied hydrocarbon	Aromatic hydrocarbon	Non-hydrocarbon	TOC (%)
26.07	3.32	11.80	5.44	5.51	21.97

Table 3
Analysis of metal elements in the oil sludge after chloroform extraction (wt.%)

Element	Weight fraction	Element	Weight fraction
Ca	8.758	Cu	0.11
Fe	5.16	Mn	0.0882
AL	3.754	Se	0.0601
Ba	2.583	Ni	0.05
K	1.369	Pb	0.0186
Na	1.237	Co	0.0164
Mg	0.4889	Cr	0.0159
Sr	0.4779	As	0.0083
Ti	0.1313	Mo	0.006
Zn	0.1285	Cd	0.0004
Total		24.4615	

TOC will be used to estimate the degradation ratio of TOC after pyrolysis.

2.3. Gaseous products analysis

The gaseous products evolved from heating process in an electrically heated fixed bed quartz reactor were analyzed by Vario Plus emission monitoring system made in Germany. The experiment system was illustrated in Fig. 1. The experiment was taken under the nitrogen atmosphere with the flow rate of 450 ml/min. Approximately, 900 mg of the as-received sample was heated from room temperature to 1027 K at the heating rate of 20 K/min.

2.4. Thermogravimetric analysis

Temperature-programmed pyrolysis experiments were performed in a TGA2050 Thermobalance. Approximately, 10 mg of the as-received samples were used for each experiment. The sample was loaded in a platinum crucible in the heated zone of TGA. A small thermocouple probe (tyke K) measured the temperature in the vicinity of the sample. The pyrolysis experiments were taken under the nitrogen atmosphere with the flow rate of 80 ml/min. The experimental results of TGA and differential thermogyavimetric (DTG) were simultaneously recorded. The pyrolysis heating rates were 10, 20 and 40 K/min, from room temperature up to 1073 K. The final solid residues were analyzed by a VAEIO EL III CNHS/O elemental analyzer with accuracy of 0.3%.

2.5. CHs evolution in pyrolysis

An oil-gas evaluation workstation (OGE-II) coupled with a flame ionization detector (FID) was employed for the quantitative analyses of hydrocarbons evolution in pyrolysis. The experimental conditions were as follows: ambient temperature, 283–303 K; ambient relative humidity ≤80%; 99.999% helium as carrier gas, its pressure was 0.20–0.30 MPa; clean air as combustion-supporting gas, its pressure was 0.30–0.40 MPa; 99.99% hydrogen as burning gas, its pressure was 0.20–0.30 MPa. There are two set of experiments were designed for different objects.

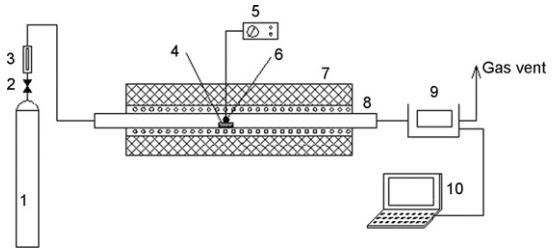

Fig. 1. Experimental system of fixed bed quartz reactor. 1. Nitrogen gas, 2. Flow regulating valve, 3. Rotameter, 4. Crucible, 5. Temperature controller, 6. Sample, 7. Electric furnace, 8. Silica tube, 9. Vario Plus emission monitoring system, 10. Computer.

2.5.1. CHs production in pyrolysis

About 100 mg oil sludge sample was used in the experiment. The hydrocarbon products in the gas can be detected by the OGE-II coupled with the FID. Firstly, the pyrolysis temperature was held at 573 K for 3 min, and then programmed from 573 to 873 K at 50 K/min and held at 873 K for 2 min. Finally, the air was introduced into the OGE-II for 6 min at 873 K; the evolved CO_2 in gas was analyzed by a thermal conductivity detector to detect the carbon residue. All experiments were conducted at least two times; the difference of the results between any two experiments needed to be less than 10%.

2.5.2. Effects of heating rates on CHs production

Around 20 mg oil sludge samples were used in experiments and helium was as carry-gas. The heating rates were 10, 20, 40 and 50 K/min, final temperature was 873 K.

3. Kinetics analysis

3.1. Model-free isoconversion method for non-isothermal experiments [17–24]

The kinetics model equation combined with the Arrhenius approach of the temperature function of reaction rate constant is expressed as:

$$\frac{d\alpha}{dt} = k_0 \exp\left(\frac{-E_\alpha}{RT}\right) f(\alpha). \quad (1)$$

where t is time (min), T the temperature (K), α the conversion of reaction W/W_∞, W the CHs weight (mg) at any temperature T, W_∞ the final CHs weight (mg), $d\alpha/dt$ the rate of reaction (min^{-1}), and $f(\alpha)$ is the reaction model. k_0, the pre-exponential factor (K^{-1}) and E_α, the activation energy (kJ/mol) are the Arrhenius parameters. R is the gas constant (kJ/mol/K). The reaction model may take various forms based on nucleation and nucleus growth, phase boundary reaction, diffusion, and chemical reaction [12,14,19,20]. However, the present investigation does not require any information of reaction model since we report here thermal decomposition kinetics using model-free approach. At a constant heating rate under non-isothermal conditions the explicit temporal/time dependence in Eq. (1) is eliminated through the trivial transformation.

$$\frac{\beta d\alpha}{dT} = k_0 \exp\left(\frac{-E_\alpha}{RT}\right) f(\alpha). \quad (2)$$

where $\beta = dT/dt$ is the heating rate (K/min) and $d\alpha/dT$ is the rate of reaction (K^{-1}).

Rearrangement and integration of Eq. (2) leads to Eq. (3) as follows.

$$g(\alpha) = \frac{k_0}{\beta}\int_0^{T_\alpha} \exp\left(\frac{-E_\alpha}{RT}\right) dT = \left(\frac{k_0}{\beta}\right) I(E, T_\alpha). \quad (3)$$

where $g(\alpha) = \int_0^\alpha [f(\alpha)]^{-1}\, d\alpha$, $I(E_\alpha, T_\alpha) = \int_0^{T_\alpha} \exp\left(\frac{-E_\alpha}{RT}\right) dT$,

Because $g(\alpha)$ is independent of heating rate, Eq. (3) can be written for a given conversion and a set of n experiments carried out at different heating rates β_i ($i = 1, \ldots, n$) as Eq. (4)

$$\left(\frac{k_0}{\beta_1}\right) I(E_\alpha, T_{\alpha,1}) = \left(\frac{k_0}{\beta_2}\right) I(E_\alpha, T_{\alpha,2}) = \cdots = \left(\frac{k_0}{\beta_n}\right) I(E_\alpha, T_{\alpha,n}). \quad (4)$$

Since the T_α values are measured with some experimental error, Eq. (4) can only be satisfied as an approximate equality. Therefore, the activation energy (E_α) can be determined at any particular value

Table 4
Expressions for some proposed approximations for the temperature integral

Author	$\int_0^T \exp(-E/RT)dT$	AAPD (%)[a]
Coats and Redfern [25]	$(RT^2/E)(1-2RT/E)\exp(-E/RT)$	0.4088
Gorbachev [26]	$(RT^2/E)[1/(1+2RT/E)]\exp(-E/RT)$	0.0917
Agrawal [27]	$(RT^2/E)[(1-2E/RT)/(1-5E/RT)]\exp(-E/RT)$	0.0085
Li [28]	$(RT^2/E)[(1-2E/RT)/(1-6E/RT)]\exp(-E/RT)$	0.0825
Starinvk $k=1.92$ [29]	$\exp(-1.0008E/RT-0.312)/(E/RT)^{1.92}$	0.3233
Cai et al. [30]	$(RT^2/E)[(E/RT+0.66691)/(E/RT+2.64943)]\exp(-E/RT)$	0.8026

[a] Average absolute percentage deviation (AAPD) from the results with direct temperature integration.

of α by finding the value of E_α for which the objective function $\Omega(E_\alpha)$ is minimized [21,22], where

$$\Omega(E_\alpha)=\sum_{i=1}^{n}\sum_{j\neq i}^{n} I\left(\frac{(E_\alpha,T_{\alpha i})\beta_j}{I(E_\alpha,T_{\alpha j})\beta_i}\right). \quad (5)$$

3.2. Numerical procedure for model-free technique

As we understand that the temperature integral in Eq. (3) has no exact analytical solution, an alternative way is to express the temperature integral by several popular approximations, the selected popular approximations are listed in Table 4.

For a set of three experiments carried out at three different heating rates (10, 20 and 40 K/min), the objective function, Ω minimization can be done by numerical method. Then the E_α can be determined at any particular value of α.

Eqs. (6) and (7) are used to compute the relative deviation (RD) and the average absolute percentage deviation (AAPD) from the direct temperature integration [24] to evaluate the accuracy of the selected approximations.

$$\mathrm{RD}(\%)=100\frac{(E_{\alpha,i}^{\mathrm{app}}-E_{\alpha,i}^{\mathrm{num}})}{E_{\alpha,i}^{\mathrm{num}}}. \quad (6)$$

$$\mathrm{AAPD}(\%)=\left(\frac{100}{N}\right)\sum_{t=1}^{N}\left|\frac{(E_{\alpha,i}^{\mathrm{app}}-E_{\alpha,i}^{\mathrm{num}})}{E_{\alpha,i}^{\mathrm{num}}}\right|. \quad (7)$$

where $E_{\alpha,i}^{\mathrm{app}}$ and $E_{\alpha,i}^{\mathrm{num}}$ are the activation energies calculated by approximations of temperature integral and direct integration method, respectively, to reach the conversion, α; N is the number of data points for each experiment.

3.3. Prediction from non-isothermal model-free analysis

The isoconversional method provides a model-free way of making kinetic predictions. The sole evaluation of E_α dependence is sufficient to simulate the non-isothermal kinetics from non-isothermal data. This is formularized [21] by Eq. (8).

$$\left(\frac{1}{\beta}\right)\int_0^{T_\alpha}\exp\left(\frac{-E_\alpha}{RT}\right)\mathrm{d}T=\left(\frac{1}{\beta_0}\right)\int_0^{T_{\alpha,0}}\exp\left(\frac{-E_\alpha}{RT}\right)\mathrm{d}T. \quad (8)$$

where β and T_α, are experimental values; $T_{\alpha,0}$ found as a solution of Eq. (8) is the temperature at which a given conversion will be reached at the arbitrary heating rate β_0 and E_α is the activation energy at a given conversion. Solving Eq. (8) for different conversions, one can predict a dependence of α on T at an arbitrary heating rate. Average relative deviation (ARD) defined by Eq. (9) is used for evaluation of the prediction deviations.

$$\mathrm{ARD}(\%)=\left(\frac{100}{N}\right)\sum_{i=1}^{N}\frac{|T_{\alpha,i}^{\mathrm{exp}}-T_{\alpha,i}^{\mathrm{pre}}|}{T_{\alpha,i}^{\mathrm{exp}}}. \quad (9)$$

where $T_{\alpha,i}^{\mathrm{exp}}$ is the experimental value of the temperature at a given α, and $T_{\alpha,i}^{\mathrm{pre}}$ is the prediction of temperature at which the given α is reached; N is the number of data points for each experiment. Since predictions using this method can be made without knowledge of the reaction model and the pre-exponential factor, they are referred as 'model-free predictions'.

4. Results and discussion

4.1. Variation of gas composition with temperature

Gas compositions of oil sludge pyrolysis in the quartz reactor are shown in Fig. 2. The quantity of the evolved gas at a temperature was obtained by integrating the area under the curves. The major gaseous products excluding N_2 are CHs (Hydrocarbons), CO_2, H_2, CO. The volume fractions of the four major gas products are 42.1, 41.5, 14 and 2.0% at 850 K and 28.5, 47.4, 15.4 and 8.6% at 1100 K, respectively. CHs mainly evolve at 650–800 K and attain a peak temperature of 740K, thereafter decay slowly till the end of experiment. More than 88% of CHs released before 850 K suggesting that the final pyrolysis temperature of 900 K is reasonable for the purposes of getting rid of the harmful organic contents and saving energy. H_2 release has a similar behavior of CHs release but with relatively minor release intensity before 850 K, there after gains another release peak at around 930 K resulting from the further cracking of heavy organic components. CO_2 release can be divided into the two stages based on the shape of evolution curve. The different mechanisms of production are expected in the two stages. First stage is mainly due to the decomposition of petroleum hydrocarbons at lower temperature (550–750 K); the second stage might be attributed to the decomposition of inorganic carbonate such as $CaCO_3$, $MgCO_3$, etc. according to Eq. (10) at higher temperature (850–1100 K). The high calcium element fraction (8.758 wt.% of inorganic matters from Table 3) in the oil sludge might further support this viewpoint. CO release mainly occurs at high temperature

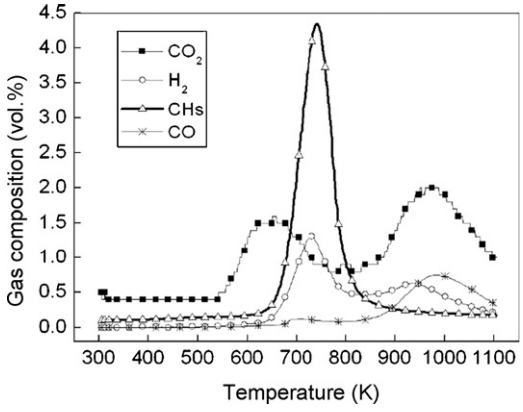

Fig. 2. Gas compositions of oil sludge pyrolysis with 20 K/min heating rate.

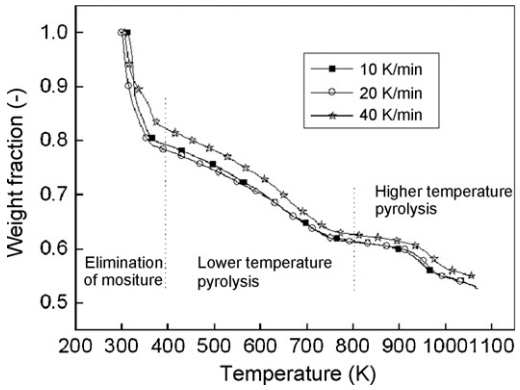

Fig. 3. TG pyrolysis curve of oil sludge samples at different heating rates.

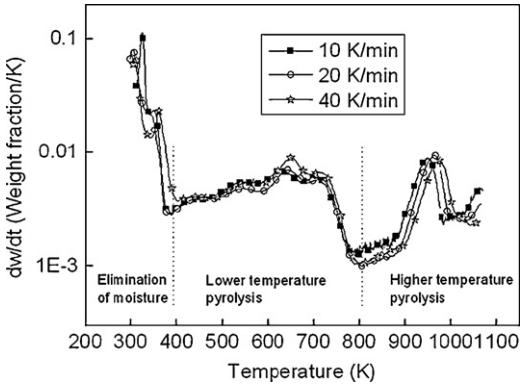

Fig. 4. DTG pyrolysis curve of oil sludge samples at different heating rates.

stage, around 78% of CO was evolved after 850 K. It is obvious that both CO_2 and CO evolved in high temperature stage are main gaseous products. Moreover the temperatures corresponding to the peak evolution of CO_2 and CO are almost the same, being 950 and 981 K, respectively. This might result from the reactions shown in Eq. (11) under the high temperature condition.

$$CaCO_3 = CaO + CO_2 \quad (10)$$

$$CO_2 + C = 2CO \quad (11)$$

4.2. Thermogravimetric analysis

Figs. 3 and 4 represent the TG and DTG curves, respectively, for the oil sludge decomposition at 10, 20 and 40 K/min heating rates. The pyrolysis yields 45–48% weight loss depending on the heating rates over the temperature range of 323–1073 K. Table 5 shows some characteristic parameters of the pyrolysis process for the three heating rates. From the shape of the TG and DTG curves (in Figs. 3 and 4), the pyrolysis process of the oil sludge can be divided into three main stages over the temperature range for all heating rates.

Table 5
TGA analysis data of the oil sludge

Heating rate (K/min)	Final weight loss (wt.%)	Lower temperature stage			Higher temperature stage
		T_{p1} (K)[a]	T_{p2} (K)[a]	T_{p3} (K)[a]	T_p (K)[a]
10	47.26	543	629	702	948
20	46.94	543	646	714	962
40	45.02	560	650	710	974

[a] Temperatures of DTG peaks (for each heating rate there are four peaks).

Table 6
Elemental analysis of solid residues at different heating rates

Heating rate (K/min)	Final solid residue (wt.%)	Elemental analysis (wt.%)				
		C	H	N	S	wt. C/H
10	52.74	3.324	0.506	0.087	1.988	6.57
20	53.06	4.098	0.394	0.138	2.230	10.40
40	54.98	4.837	0.316	0.096	2.577	15.31

4.2.1. Elimination of moisture stage

A first period of mass decrease is registered before 393 K. The weight loss in this stage is 18–20 wt.% of the original weight; the proximate analysis shows that there is 16.95 wt.% of moisture in the oily sludge, so it can be expected that the major fraction of weight loss is mainly related to the evaporation of moisture, although volatile compounds can contribute to the weight loss.

4.2.2. Lower temperature stage of pyrolysis

A second stage of mass decrease is observed between 393 and 805 K and involves a very important weight loss (around 18 wt.% of the original weight) mainly related to volatilization and decomposition of organic matters in the oil sludge (from Fig. 2). Apparently, only slight difference between the pyrolysis behaviors of the oil sludge at the 10 and 20 K/min heating rates is observed in this stage. One explanation could be that the difference between the two heating rates is not large enough to significantly affect the pyrolysis behavior. However, with the 40 K/min heating rate, the difference in the pyrolysis behavior can be observed. That is both the maximum weight loss rate and pyrolysis residue at 805 K are high compared with those at 10 and 20 K/min. Fig. 4 shows that the weight loss is significant in range of 473–773 K. The DTG curves at this stage are characterized by containing several peaks. The possible reason of the multi-peak might be attributed to the complex compositions having different boiling points and physical or chemical property in the sludge [2].

4.2.3. Higher temperature stage of pyrolysis

A third stage of mass decrease is observed between 805 and 1023 K with a relatively small weight loss (around 7.5 wt.% of the original weight). The temperature corresponding to maximum weight loss rate in this stage is at 950–975 K. The weight loss of oil sludge in this temperature range might be mainly attributed to the decomposition of inorganic materials calcium (such as $CaCO_3$, $MgCO_3$, etc.) based on the above analysis in Section 4.1. It was observed that the final pyrolysis residue is approximately 53–55 wt.% of the original weight, which is consistent with the sum of fixed carbon and ash from the proximate analysis results (Table 1). Higher heating rate leads to a higher fraction of final solid residue (see Table 6), the elemental analysis of the final solid residues indicates that higher heating rate increases the carbon (C) and sulfur (S) contents but decreases hydrogen (H) content in solid residues. The weight ratio of C/H in solid residues shows an increasing trend with increasing heating rate.

4.3. CHs production in pyrolysis

The quantitative analysis about the yield of CHs in pyrolysis was conducted according to the purposely non-linear heating procedure (see Section 2.5.1) by using OGE-II. Table 7 shows that the yield of CHs during temperature was held at 573 K for 3 min (S_1) is 88.24 mg/g; the yield of CHs from 573 to 873 K and then hold at 873 K for 2 min (S_2) is 144.46 mg/g; the carbon residue (S_3) is relatively small (43.87 mg/g), about 80.3% of TOC is converted into CHs ($S_1 + S_2$) in the pyrolysis. This is consistent with the result by the

Table 7
CHs production in pyrolysis

S_1 (mg/g)	S_2 (mg/g)	S_3 (mg/g)	D (%)[a]
88.24	144.46	43.87	80.03

[a] Degradation ratio of TOC = $100(1 - S_3/10\ \text{TOC})$.

Schmidt and Kaminsky [11] who pyrolyzed oil sludge in a fluidized bed at temperatures from 733 to 823 K and separated 70–84% of the oil from the oil solids.

4.4. Effects of heating rates on CHs evolution

To understand the effect of heating rates on CHs production, the pyrolysis experiment at different heating rates were carried out by an OGE-II coupled with FID. The detailed information was reported through Figs. 5 and 6. The initial weight of samples (W_0), the temperatures corresponding to the peak intensity of CHs evolution (T_{m1}, T_{m2}), and the temperature at 90% CHs conversion ($T_{90\%}$) are reported in Table 8 for each case of the experiments.

Fig. 5 shows that the CHs evolution is significant in the range of 600–723 K; the heating rates present an important influence on conversion of CHs in pyrolysis. Higher heating rate causes the peak intensity of CHs evolution to increase. The temperatures corresponding to the maximum evolution rate of CHs are 678, 691,705 and 705 K at different heating rates of 10, 20, 40 and 50 K/min, respectively. The conversions of CHs with temperatures in pyrolysis at different heating rates are reported through Fig. 6. Fig. 6 shows that the CHs evolution at higher heating rate shifts to a high-temperature region with different extent depending on the heating

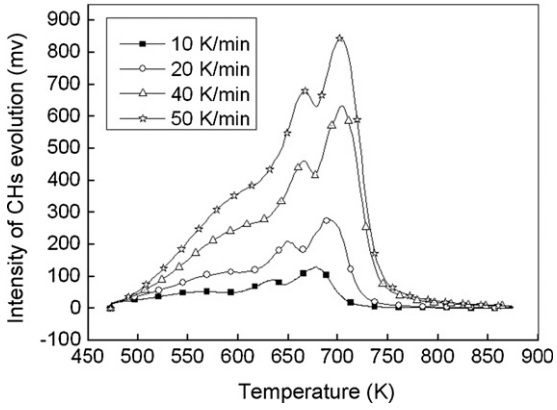

Fig. 5. Intensity of CHs evolution with temperature at different heating rates.

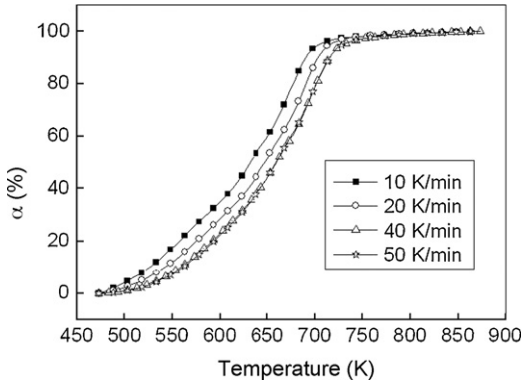

Fig. 6. Conversion of CHs with temperature at different heating rates.

Table 8
Analysis data on CHs evolution in pyrolysis for different heating rates

Heating rate (K/min)	W_0 (mg)	I_{max} (mv)[a]	T_{m1} (K)[b]	T_{m2} (K)[b]	$T_{90\%}$ (K)[c]
10	21.7	124	635	678	691
20	20.6	280	649	691	704
40	20.5	632	665	705	716
50	22.3	845	667	705	717

[a] Maximum intensity of CHs evolution.
[b] Temperature corresponding to the peak intensity of CHs evolution.
[c] Temperature at 90% conversion of CHs.

rates. For the experiments conducted at the 10, 20 and 40 K/min heating rates, this shift is obvious. However for the experiments at the 40 and 50 K/min heating rates, only a slight shift is observed. This can be explained on the basis of heat transfer and medium diffusion. For the lower heating rates experiments, generally the pyrolysis experiment at higher heating rate has shorter reaction time (in the same temperature region), the evolution is shifted to higher temperature. However the thermal resistance and the diffusion resistance might be too small to be a main factor to significantly affect the CHs conversion behavior from 40 to 50 K/min.

The comparison of CHs evolution between Figs. 2 and 5 shows that the temperature delay of around 50 K was formed in the experiment system illustrated in Fig. 1, this is due to the transmission of gas from the reactor to the gas analysis system.

4.5. Kinetics for non-isothermal model-free analysis

Application of the model-free isoconversional method to the non-isothermal decomposition of oil sludge samples to obtain activation energy (E_α) dependency on conversion (α) using direct numerical temperature integration [24] is presented through Fig. 7. It is observed from Fig. 7 that E_α is an increasing function of α in overall CHs evolution process, it increases from 46 to 111 kJ/mol at α = 6–94%. The increasing E_α with α indicates that the reaction corresponding to the CHs evolution at lower temperature takes place much easier than that at higher temperature.

According to basic kinetics concepts, a variation of kinetic parameters implies a variation in the mechanism that controls the pyrolysis. The E_α-dependence on the extent of conversion reveals the kinetic complexity in the multi-step processes. From the $dE_\alpha/d\alpha$ curve in Fig. 7, variation of E_α with α can be divided into two stages at α = 50%. The pyrolysis temperatures at α = 50% under different heating rates are 631, 647 and 660 K (from Fig. 6); these

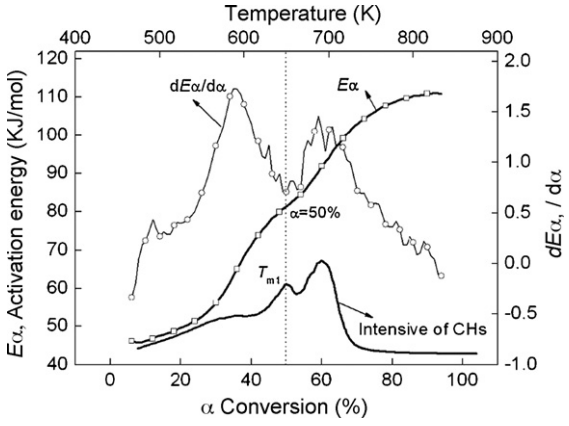

Fig. 7. Dependency of activation energy on conversion of non-isothermal decomposition of oil sludge at 10, 20 and 40 K/min heating rates using direct numerical temperature integration.

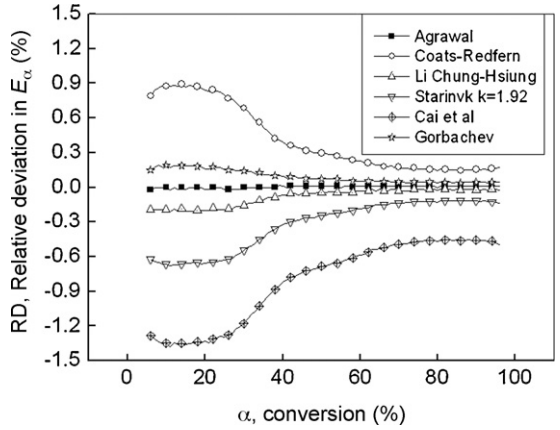

Fig. 8. Relative deviation from direct integration.

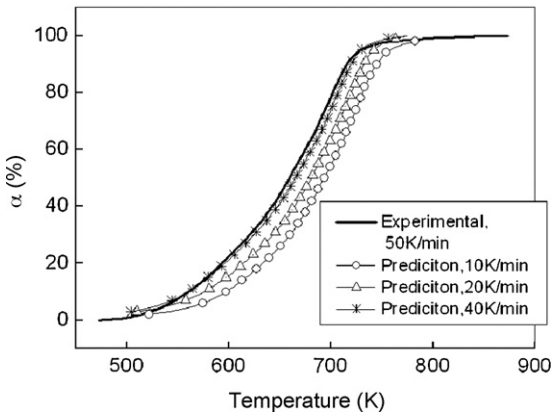

Fig. 9. Prediction of dependence of α on T at 10, 20 and 40 K/min heating rates using the direct integration for 50 K/min heating rate.

temperatures are in accordance with the first peak temperatures of CHs evolution (T_{m1} in Table 8). In order to reflect the corresponding relation between the variation of E_α and CHs evolution, the intensive of CHs evolution at the heating rate of 20 K/min was also plotted in Fig. 7. Previous study [32] by using differential scanning calorimetry (DSC) and thermogravimetry (TG/DTG) has indicated that the pyrolysis process of six crude oils indicated two main temperature ranges where loss of mass was observed. The first region between ambient and 673 K was distillation. The second region between 673 and 873 K was visbreaking and thermal cracking. This point was also mentioned by Ciajolo and Barbella [33] in early years. The study on pyrolysis of API oil sludge [2] has further firmed that the weight loss at low temperature (around 523 K) was in fact resulted from the volatilization, the main pyrolysis (or thermal cracking) for the sludge takes place between 688 and 713 K depending on the heating rates. Thus, one might believe that the reactions for α of 0–50% are mainly contributed by volatilization of light CHs in the oil sludge; the strong and increasing E_α dependency on α (for $\alpha < 50\%$) might be mainly associated with the increasing boiling point of the light CHs in oil sludge. The reactions for α of 50–100% are mainly contributed by thermal cracking of heavy CHs in oil sludge; the relatively slow but increasing E_α dependency on α in the later stage ($\alpha > 50\%$) is possibly associated with the stronger linked hydrocarbon molecules at higher conversion stage, because the weak linked ones have been consumed at previous steps for a multi-step reaction processes. The arithmetic mean activation energy for the first stage ($6\% < \alpha < 50\%$) is 59.59 kJ/mol, for the second stage ($50\% < \alpha < 95\%$) is 102.02 kJ/mol.

E_α dependency on α using several popular approximations used for integration of Eq. (3) was also calculated to evaluate the accuracy of these approximations. The CHs evolution reaction occurs for $10 < E/RT < 20$. The selected approximations showed almost similar results. Their relative deviations (RD) from the results with direct integration were evaluated and are presented in Fig. 8. This figure shows that the higher deviation mainly occurs for $\alpha < 50\%$, the accuracy of approximations are better than 0.3% for $\alpha > 50\%$ except the new approximation of Cai et al. The most accurate approximation is Agrawal's approximation with the average absolute percentage deviation (AAPD) of 0.0085%; its high accuracy has been verified by several studies [17,24,27,30]. However the new approximation of Cai et al. is inferior to all other approximations with the maximum AAPD of 0.802%.

The obtained E_α dependency derived from non-isothermal data is used to simulate another non-isothermal kinetics data using the direct temperature integral. The simulation result agrees well with the experimental data. Fig. 9 shows the results of predictions as compared to actual non-isothermal measurement conducted at 50 K/min heating rate. Results show that the ARD values are 5.63, 3.60 and 1.32%, respectively, for heating rates 10, 20 and 40 K/min. The E_α dependency from non-isothermal data has shown reliable prediction of other non-isothermal data.

5. Conclusions

Pyrolysis of tank bottom oil sludge was studied. The pyrolysis reaction is significant in the range of 473–773 K where multi-peak DTG curves can be gained. The heating rates have a relative effect on the oil sludge pyrolysis. As the heating rate increases, the total volatile matter evolved decreases and the DTG peaks shift to higher temperature. Higher heating rate increases the carbon (C) and sulfur (S) contents but decreases hydrogen (H) content in solid residues. The major gaseous products excluding N_2 are CHs (Hydrocarbons), CO_2, H_2, CO. The yield of CHs in pyrolysis is significant in the range of 600–723 K, and can be influenced by heating rate distinctly. Higher heating rate causes the peak intensity of CHs evolution to increase and the CHs evolution to move towards a high-temperature region. Around 80% of TOC in the oil sludge can be converted into CHs in pyrolysis process.

Application of model-free isoconversional method to non-isothermal decomposition of oil sludge samples to obtain activation energy (E_α) dependency on conversion (α) in the pyrolysis of oil sludge is calculated by numerical method. The variation of E_α with α can be divided into two stages at $\alpha = 50\%$ based on the $dE_\alpha/d\alpha$ curve and the physical or chemical property of the sludge. The arithmetic mean activation energies for the two stages are 59.59 and 102.02 kJ/mol, respectively. The obtained E_α dependency derived from non-isothermal data is used to simulate another non-isothermal kinetics data using the direct temperature integral. The simulation result agrees well with the experimental data with ARD values of 5.63, 3.60 and 1.32%, respectively, for heating rates 10, 20 and 40 K/min.

Acknowledgements

This work was supported by the National High Technology Research and Development Program of China (863 Program) (Grant no. 2007AA05Z333), and China Postdoctoral Science Foundation (Grant no. 20070410177).

References

[1] Guidance Manual for Hazardous Waste Permits, U.S. Environmental Protection Agency Office of Solid Waste and Emergency Response, PB 84-10057, Washington, DC, 1989.
[2] P. Punnaruttanakun, V. Meeyoo, C. Kalambaheti, P. Rangsunvigit, T. Rirksomboon, B. Kitiyanan, Pyrolysis of API separator sludge, J. Anal. Appl. Pyrolysis 68–69 (2003) 547–560.
[3] J.L. Shie, C.Y. Chang, J.P. Lin, C.H. Wu, D.J. Lee, Resources recovery of oil sludge by pyrolysis: kinetics study, J. Chem. Technol. Biotechnol. 75 (2000) 443–450.
[4] C.Y. Chang, J.L. Shie, J.P. Lin, C.H. Wu, D.J. Lee, C.F. Chang, Major products obtained from the pyrolysis of oil sludge, Energy Fuels 14 (2000) 1176–1183.
[5] J.L. Shie, C.Y. Chang, J.P. Lin, D.J. Lee, C.H. Wu, Use of inexpensive additives in pyrolysis of oil sludge, Energy Fuels 16 (1) (2002) 102–108.
[6] J.L. Shie, J.P. Lin, C.Y. Chang, C.H. Wu, D.J. Lee, C.F. Chang, Y.H. Chen, Kinetics of the oxidative thermal treatment of oil sludge at low heating rates, Energy Fuels 18 (2004) 1272–1281.
[7] J.L. Shie, J.P. Lin, C.Y. Chang, D.J. Lee, C.H. Wu, Pyrolysis of oil sludge with additives of sodium and potassium compounds, Resour. Conserv. Recycl. 39 (2003) 51–64.
[8] J.L. Shie, J.P. Lin, C.Y. Chang, S.M. Shih, D.J. Lee, C.H. Wu, Pyrolysis of oil sludge with additives of catalytic solid wastes, J. Anal. Appl. Pyrolysis 71 (2004) 695–707.
[9] J.L. Shie, C.Y. Chang, J.P. Lin, D.J. Lee, C.H. Wu, Thermal degradation kinetics of oil sludge in the presence of carbon dioxide, J. Chin. Inst. Environ. Eng. (Taiwan) 11 (4) (2001) 307–316.
[10] Z. Wang, Q. Guo, X. Liu, C. Cao, Low temperature pyrolysis characteristics of oil sludge under various heating conditions, Energy Fuels 21 (2007) 957–962.
[11] H. Schmidt, W. Kaminsky, Pyrolysis of oil sludge in a fluidised bed reactor, Chemosphere 45 (2001) 285–290.
[12] S. Vyazovkin, C.A. Wight, Model-free and model-fitting approaches to kinetic analysis of isothermal and nonisothermal data, Thermochim. Acta 340–341 (1999) 53–68.
[13] C.D. Doyle, Kinetic analysis of thermogravimetric data, J. Appl. Polym. Sci. 5 (1961) 285–292.
[14] S. Vyazovkin, D. Dollimore, Linear and nonlinear procedures in isoconversional computations of the activation energy of nonisothermal reactions in Solids, J. Chem. Inf. Comp. Sci. 36 (1996) 42–45.
[15] S. Vyazovkin, Advanced isoconversional method, J. Therm. Anal. 49 (1997) 1493–1499.
[16] L.F. Calvo, M. Otero, B.M. Jenkins, A.I. García, A. Morán, Heating process characteristics and kinetics of sewage sludge in different atmospheres, Thermochim. Acta 409 (2004) 127–135.
[17] B. Saha, A.K. Maiti, A.K. Ghoshal, Model-free method for isothermal and nonisothermal decomposition kinetics analysis of PET sample, Thermochim. Acta 444 (2006) 46–52.
[18] S. Vyazovkin, V. Goriyachko, Potentialities of software for kinetic processing of thermoanalytical data by the isoconversion method, Thermochim. Acta 194 (1992) 221–230.
[19] S. Vyazovkin, Computational aspects of kinetic analysis. Part C. The ICTAC Kinetics Project—the light at the end of the tunnel? Thermochim. Acta 355 (2000) 155–163.
[20] S. Vyazovkin, C.A. Wight, Kinetics of thermal decomposition of cubic ammonium perchlorate, Chem. Mater. 11 (1999) 3386–3393.
[21] S. Vyazovkin, A unified approach to kinetic professing of nonisothermal data, Int. J. Chem. Kinet. 28 (1996) 95–101.
[22] S. Vyazovkin, N. Sbirrazzuoli, Isoconversional kinetic analysis of thermally stimulated processes in polymers, Macromol. Rapid Commun. 27 (2006) 1515–1532.
[23] J.D. Peterson, S. Vyazovkin, C.A. Wight, Kinetics of the thermal and thermooxidative degradation of polystyrene and poly (propylene), Macromol. Chem. Phys. 202 (2001) 775–784.
[24] B. Saha, A.K. Ghoshal, Model-free kinetics analysis of waste PE sample, Thermochim. Acta 451 (2006) 27–33.
[25] A.W. Coats, J.P. Redfern, Thermal studied on some metal complexes of hexamethy leniminecarbodithioate, Nature 1 (1964) 68–69.
[26] V.M. Gorbachev, A solution of exponential integral in the nonisothermal kinetics for linear heating, J. Therm. Anal. Calorim. 8 (1975) 349–350.
[27] R.K. Agrawal, Integral approximation for nonisothermal kinetics, AIChE J. 33 (1987) 1212–1214.
[28] C.H. Li, An integral approximation formula for kinetic analysis of nonisothermal TGA data, AIChE J. 31 (1985) 1037–1038.
[29] M.J. Starink, A new method for the derivation of activation energies from experiments performed at constant heating rate, Thermochim. Acta 288 (1996) 97–104.
[30] J. Cai, F. Yao, W. Yi, F. He, New temperature integral approximation for nonisothermal kinetics, AIChE J. 52 (2006) 1554–1557.
[31] http://www.jl2sy.cn/chuying_huanbao/law/L0000093.htm.
[32] M.V. Kök, O. Karacan, Pyrolysis analysis and kinetics of crude oils, J. Therm. Anal. Calorim. 52 (3) (1998) 781–788.
[33] A. Ciajolo, R. Barbella, Pyrolysis and oxidation of heavy fuel oils and their fractions in a thermogravimetric apparatus, Fuel 63 (1984) 657–661.